Electrical Power and Energy Systems 121 (2020) 106060

Contents lists available at ScienceDirect

Electrical Power and Energy Systems

journal homepage: www.elsevier.com/locate/ijepes

Coordinating energy management for multiple energy hubs: From a transaction perspective

Xiaodi Wang[a], Youbo Liu[a,*], Chang Liu[b], Junyong Liu[a]

[a] College of Electrical Engineering, Sichuan University, Chengdu, China
[b] State Grid Sichuan Electric Power Research Institute, Chengdu, China

ARTICLE INFO

Keywords:
Energy hubs
Decentralized optimization
P2P transaction

ABSTRACT

The coupled multiple energy carriers integrated with distributed energy units, e.g., energy converters, renewable energy, and storages have offered energy hubs high flexibility and independent controllability. In this paper, a decentralized transactive based energy management framework enabling coordination among multiple energy hubs (MEHs) is developed. Aiming to improve the economic performance of the interconnected energy hub system, a peer to peer (P2P) transaction platform is established for the self-organized trading of MEH. Particularly, a generic scheme for the generation of transaction prices is specified for the energy hub, which is firstly integrated into a modified alternating direction method of multipliers (ADMM) method for the realization of achieving P2P transaction consensus amongst MEHs. Furthermore, this price scheme offers high traceability of energy-price flows inner EHs operation process and external energy transaction activities, providing transparent price signals in the local P2P market. A three-energy hub system is simulated, and numerical case studies have demonstrated the proposed coordination scheme actively encourages individual EH to enroll in the P2P transaction scheme, offering all EHs a win-win transaction framework and improving the global economic efficiency of the networked system.

1. Introduction

The technology development in energy industry has significantly accelerated the pace of the energy transition by exploiting the synergy of various energy carriers, e.g., electricity, heat and gas [1]. Energy hub (EH), a paradigmatically ensemble device combining a variety of distributed energy units, has been proposed in decade to address the challenge of multi-energy systems (MES) management. The implementation of EH, as reported in [2], enables the activation of energy exchange as well as information interaction among the stakeholders in multi-energy balance, which is especially applicable for MES in building and district.

In this decade, the growing efforts have been devoted to investigating the operation and schedule optimization for the EH integrated with multiple-energy resources in a certain area. For example, reference [3] proposed a multi-objective dispatching framework to optimize cost-emission and economic operation for the EH considering demand response. A modified gravitational search method based on self-adaptive learning strategy was employed for EH economic dispatch in [4]. In addition, a general stochastic model was formulated to handle the adverse impact of intermittent wind power integrated in the smart EH in [5]. From the perspective of market participating strategy, a day-ahead decision model was established in [6] to enable a receding horizonal optimization of MES including heat, gas, cooling and electricity. In [7], a market transaction method was presented to assist the EH operator in determining their optimal involvements in upstream wholesale energy markets while simultaneously considering the optimum pricing of electricity and heat services provided to its end-users. However, the similar researches neglected the revelation of price signals accurately reflecting the time-varying balance conditions among EHs as well as their individual trading strategies.

In addition, the majority of studies in this field focused on addressing the challenge of realizing the robust and beneficial energy scheduling in the presence of the undesired uncertainties, e.g., the variable prices, uncontrollable demands, and stochastic renewable outputs. The renewable energy output and load demand of geographically adjacent areas can be diverse and complementary [8]. In this respect, the networked multiple energy hub (MEH) system shows its promising advantage to handle this issue. Particularly, the diversity of EH configurations and demand patterns may lead to significant economic difference in energy conversion and production. Thus, the geographically dispersed MEHs, connected by local energy networks, can

* Corresponding author.
E-mail address: liuyoubo@scu.edu.cn (Y. Liu).

https://doi.org/10.1016/j.ijepes.2020.106060
Received 3 January 2020; Received in revised form 10 March 2020; Accepted 30 March 2020
Available online 22 April 2020

Nomenclature

Variables

v_{fi}	Dispatch factor for converter unit *i* connected to the input energy *f*.
P_f^c/P^s	Imported/exported energy carrier *f* from/to the upstream utilities
P_k^{ch}/P_k^{dis}	Charging/discharging energy of ESS k
P_{ij}^{unit}	Output energy of converter i for energy carrier j
P_j^{node}	Collected energy at collector nodes for energy carrier j
$P_{n,j}^{ex}$	Exported energy from EH n to other EHs for energy carrier j
$P_{nm,j}^{im}$	Imported energy for EH n from EH m for energy carrier j without considering the transmission loss
$P_{nm,j}^{im'}$	Imported energy for EH n from EH m for energy carrier j with considering the transmission loss
π_k^{ESS}	The operation cost of ESS k
π_i^{unit}	The operation cost of converter i
π_j^{trade}	The operation cost of trading energy carrier j
$\boldsymbol{v_n}$	Dispatch matrix of EH n
$\boldsymbol{P_n^C}$	Vector of input energy carriers of EH n
$\boldsymbol{x_n}$	Concatenated decision vector of EH n
SOC_k	Energy capacity of storage *k*
C_k^{SOC}	Price of stored energy in storage *k*
C_k^{ESS}	Price of charging/discharging energy of ESS k
C_{ij}^{unit}	Price of output energy of converter i for energy carrier j
C_j^{node}	Price of output energy of the collector node for energy carrier j
C_j^L	Price of output energy of EH for energy carrier j
$P_{nm,j}^{loss}$	Transmission loss for EH n importing energy from EH m
$E1_n$	The operation cost of EH n
$E2_n$	The transaction cost of EH n with the upstream utilities
$E3_n$	The transaction cost of EH n with the networked EHs
h_j	Constraint of the EH interconnection network for energy carrier j
g_n	Constraint of the physical control scheme of EH n
$\boldsymbol{z_n}$	Set of auxiliary variable vector of the ADMM.

Parameters

$\eta_{n,ij}^c$	Converter efficiency for converter i to converter energy carrier j in EH n
$P_{n,j}^L$	load demands for energy carrier j in EH n
$P_{n,j}^{rew}$	Renewable energy output for energy carrier j in EH n
SOC^{max}	Maximum stored energy of ESS
SOC^{min}	Minimum stored energy of ESS
l_{nm}	Energy transmission loss between EH n and EH m
α_i, β_i	Operation cost coefficients for converter
α_k	Operation cost coefficients for ESS
α_j	Operation cost coefficients for transaction
η_n	Conversion matrix of EH n
$P_n^{unit,up}$	Maximum units converting energy
$P^{im,up}$	Maximum imported energy
$P^{ex,up}$	Maximum exported energy
$P^{dis,up}$	Maximum discharged energy of ESS
$P^{ch,up}$	Maximum charged energy of ESS
C^c/C^s	The price of imported /exported energy from/to upstream utilities
S_{jk}	Storage coupling element
ε	converge threshold
P_n^L	Vector of load demands of EH n

Set

Ξ^N	Set of EH systems
$\Xi^{\mathcal{N}_n}$	Set of EHs connected with EH n
Ξ^J	Set of EH output energy carriers
Ξ^F	Set of input energy carriers to EH
Ξ^I	Set of input energy carriers to energy converter units at the EH input junctions
Ξ^K	Set of EH energy storage systems
Ξ^T	Set of hours of the scheduling horizon

Index

n	Index of EH
j	Index of EH output energy carriers
f	Index of EH input energy carriers
τ	Index of iteration
i	Index of converter units at the EH input junctions
k	Index of EH energy storage
t	Index of hour

be controlled and dispatched coordinately to improve the whole system efficiency. The coordinated operation paradigm can be generally considered as an optimal energy flow (OEF) problem for the networked EHs and external MES. Ideally, the centralized solver has been proved to be effective for the coordination problem in a number of studies [9]. However, the centralized dispatch framework usually requires the global deployment of sensors and communication infrastructure as well as the sufficient details of the included elements. Also, the local decisions and operation strategies of different stakeholders are not encouraged in the centralized dispatch methods, which can result in local privacy and welfare loss. Moreover, the computing intractability in solving the global OEF issues might occur with the growth of system scale and optimization dimension [10]. All these deficiencies hinder the centralized coordination scheme from being realistically employed in dealing with the large-scale coordination issue.

To address these challenges, recent literatures have shown the increasing interest for the autonomous energy coordination of the networked self-governed entities. Different transaction structures for local-centric markets are discussed in [11], from auction-based structures [12] to full peer-to-peer (P2P) mechanism [13] implemented at the micro-grid (MG) level. Particularly, double auction-based energy transaction scheme for electric vehicles and MGs were respectively discussed in [14,15] aiming at improving the economic benefits of individual agents. While in [16], the authors presented a bilevel stochastic programming algorithm based on the alternating direction method of multipliers (ADMM) to guarantee the convergence of operation decisions of networked MGs through distributed iterations. Moreover, a dual sub gradient algorithm was introduced in [17] to coordinate MGs operation in [17]. And in order to reveal the market equilibrium process of decentralized trading, a Nash bargaining framework among the connected MGs was proposed in [18], in which a standard ADMM method was applied to decompose and solve the problem. Reference [14,18] enabled coordination optimization among the distributed MGs by exploiting the complementary potential of supply and demand locating at disperse areas. However, those works have not emphasized the studies on formulating an effectively autonomous pricing mechanism that is highly applicable for distributed MEH. The transactive decision reference derived from price signals is particularly important in the commercialized energy trading, which therefore needs to be specifically focused.

Accordingly, the distributed and consensus-based algorithms were further investigated for maturing the sophisticated decentralized transaction scheme. The concept of a transactive energy (TE) control mechanism for coordinated networked microgrids was proposed in [19], where the provision of clear price signals facilitating the market fairness of distributed participants was claimed. Aiming at reaching a consensus on ultimate transaction prices, Some works [20,21] adopted a modified ADMM or dual gradient algorithm for P2P trading by introducing dual variables to represent the transaction prices for each MG, i.e., the electricity selling price and buying price. Thus, the connected MGs are capable to reach a final consensus on the ultimate P2P transactive energy by iteratively updating the price variables following a particular gradient. By doing so, the supply-demand status of market balance could be disclosed in a certain extent, but, still, the inner operational cost of each entity failed to be effectively considered. Moreover, as it comes to EHs, two other aspects ought to be considered in terms of the design of transaction pricing mechanism: (1) EH operation cost is highly affected by its operation scheme due to its non-ideal conversion, storage process. Thus, the EH operation scheme differentiation can yield transaction price differentiation [22]; (2) EH, integrated within MES, of which the determined transaction prices are tightly coupled for various energy carriers to meet the load and transaction demand. However, these two aspects have not been thoroughly investigated so far. In this regard, the decentralized methods proposed by [20,21] might be inapplicable for MEH system. On the one hand, its local P2P market processes without consideration of operation cost, which can produce misleading transaction price signals and lead to individual benefit loss at the real-time operation scheme. On the other hand, the coupling relationship among multi-energy carriers are ignored, which can bring significant difference in ultimate generated transaction prices among all entities.

To cope with the aforementioned challenges, a TE based coordination framework for MEHs is proposed in this paper. Specifically, we emphasize on a practical framework to provide the energy price signals in the holistic P2P procedure to encourage the autonomously collaborative actions among the distributed EHs. The proposed P2P scheme plays as a market-based decentralized mechanism that drives EHs to participate in the trading interactions through the iterative value-based information-exchange. The main contributions of the work can be summarized as below:

(1) In this paper, a novel price generation scheme coupling heat/electricity balance of MEH is presented and firstly integrated into an improved ADMM algorithm to achieve the coordination of the networked MEHs. Specifically, the transactive prices of each EH is directly derived based on its unit configuration, inner operation strategy, and trading policy, which effectively guide the transactive energy flow among EHs to achieve the global optimum with full respect of local decisions.
(2) The generic model is proposed enabling dynamic tracing of energy-price flows in EHs and external energy transactions. The model readily reflects the traceability of EHs operation and, meanwhile, offers a highly scalable tool to assist decentralized MEH in establishing business paradigm applicable for diverse types of EHs.
(3) The P2P transactive framework proposed in this paper outperforms the traditionally distributed optimization algorithm in terms of the provision of dynamic and transparent price signals. This decentralized mechanism empowers the included EHs to actively coordinate with each other for local benefit, and meanwhile improve the whole system welfare.

The rest paper is organized as follows: Section 2 introduces the generic model of individual EH. Section 3 provides the mathematical methodology to characterize the coordination process for MEH based on centralized and decentralized P2P transaction optimization concepts. In Section 4, numerical cases studies are carried out to validate the proposed market structure. And section 5 concludes the study and discusses the future work

2. The general modeling formulation of EH system

2.1. Energy hub model

An energy hub generally imports energy from the upstream network utilities e.g., electricity, natural gas, or heat networks. The imported energy will be converted by the EH inside units, and then consumed by its actual loads [23] or provided for the outside system. The schematic configuration of a typical EH is illustratively given by Fig. 1, and the general formulation of EH n can be presented as:

$$\underbrace{\begin{bmatrix} P_{n,1}^L \\ P_{n,2}^L \\ \vdots \\ P_{n,J}^L \end{bmatrix}}_{P_n^L} = \underbrace{\begin{bmatrix} \eta_{n,11}^c & \eta_{n,12}^c & \cdots & \eta_{n,1I}^c \\ \eta_{n,21}^c & \eta_{n,22}^c & \cdots & \eta_{n,2I}^c \\ \vdots & \vdots & \ddots & \vdots \\ \eta_{n,j1}^c & \eta_{n,j2}^c & \cdots & \eta_{n,jI}^c \end{bmatrix}}_{\eta_n} \times \underbrace{\begin{bmatrix} \nu_{n,11} & \nu_{n,12} & \cdots & \nu_{n,1F} \\ \nu_{n,21} & \nu_{n,22} & \cdots & \nu_{n,2F} \\ \vdots & \vdots & \ddots & \vdots \\ \nu_{n,I1} & \nu_{n,I2} & \cdots & \nu_{n,IF} \end{bmatrix}}_{\nu_n} \times \underbrace{\begin{bmatrix} P_{n,1}^C \\ P_{n,2}^C \\ \vdots \\ P_{n,F}^C \end{bmatrix}}_{P_n^C} \tag{1}$$

The received energy $\boldsymbol{P_n^C}$ from network utilities at the input ports of the EH n will be dispatched by EH operator towards the converters, of which the dispatching process can be expressed as dispatch matrix $\boldsymbol{\nu_n}$. Then, the dispatched energy into each converter unit in the EH (e.g., CHP, micro-turbine) will be converted with corresponding efficiencyη_n^c to satisfy the load demands $\boldsymbol{P_n^L}$. Thus, the conversion matrix $\boldsymbol{\eta_n}$ in the EH can be formulated accordingly. Note that zero efficiency value in conversion matrix $\boldsymbol{\eta_n}$ means that no associated energy converters have been equipped inside the EH.

Moreover, in the presence of installed renewable energy generators, energy storage system (ESS) and the transaction demand of

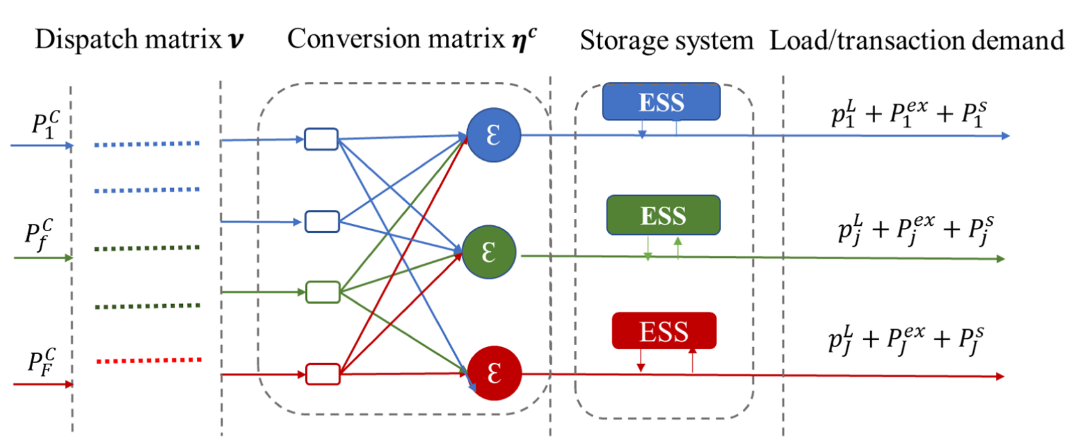

Fig. 1. Schematic configuration of a typical EH.

interconnected EHs, the detailed energy balance constraint of EH n at time plot t can be descripted as (2).

$$P^{L}_{n,jt} = \sum_{i\in\Xi^I}\left(\eta^{c}_{n,ij}\cdot\sum_{f\in\Xi^F}(v_{n,fit}\cdot P^{c}_{n,ft})\right) - P^{s}_{n,jt} + \sum_{k\in\Xi^K} S_{n,jk}\cdot(P^{dis}_{n,kt} - P^{ch}_{n,kt}) + \sum_{m\in\Xi^{\mathcal{N}_n}} P^{im}_{nm,jt} - P^{ex}_{n,jt} + P^{rew}_{n,jt}\ \forall j\in\Xi^J;\ \forall t\in\Xi^T;\quad \forall n\in\Xi^N \tag{2}$$

where Ξ^F, Ξ^I, Ξ^K, Ξ^J are the set of input energy carriers, converter units, ESS and output energy carriers of EH $n \in \Xi^N$respectively. The element S_{jk} maps the energy flow between storage k and output energy carrier j ($S_{jk} \in \{0, 1\}$). $P^{im}_{nm,j}$ denotes EH n imports energy j from EH $m \in \Xi^{\mathcal{N}_n}$and $\Xi^{\mathcal{N}_n}$ is a set of EHs adjacent to EH n with connected energy transmission network.

In general, the EH load demand can be supplied by the following four energy resources: (1) the energy imported from the upstream network utilities; (2) the stored energy in the ESS; (3) the transaction energy from networked EH systems; and (4) the output energy from equipped renewable energy generator P^{rew}_{n}. In this regard, the decision vector of EH $n \in \Xi^N$at each time plot t can be expressed as $\boldsymbol{x}_n = [[P^c_f]_{f\in\Xi^F}, [v_{fit}]_{f\in\Xi^F, i\in\Xi^I}, [P^{ch}_{n,k}, P^{dis}_{n,k}]_{k\in\Xi^K}, [P^{ex}_{n,j}, P^{s}_{n,j}]_{j\in\Xi^J}, [P^{im}_{nm,j}]_{j\in\Xi^J, m\in\Xi^{\mathcal{N}_n}}]$.

2.2. EH output price

EH operation scheme is highly affected by a series of factors, e.g., the energy prices of the upstream utilities, load demands, renewable energy output and its transaction decisions. Besides, the EH energy prices for various energy carriers are tightly coupled and affected by the EH operation process. Thus, different EH operation scheme can bring different output energy prices [22]. A generic model is proposed here to detailly analyze the EH output energy price, enabling dynamic tracing of energy-price flows at each operation step of an EH system.

(1) **Converter output energy price**

A non-ideal converter inside the EH will convert energy with certain energy loss. Considering each converter's conversion efficiency, the output energy flow $p^{unit}_{n,ijt}$ at each converter's output port for the output energy carrier j can be calculated as below:

$$p^{unit}_{n,ijt} = \eta^{c}_{n,ij}\cdot\sum_{f\in\Xi^F}(v_{n,fit}\cdot P^{c}_{n,ft})\ \forall i\in\Xi^I;\quad \forall j\in\Xi^J;\ \forall n\in\Xi^N;\ \forall t\in\Xi^T \tag{3a}$$

Thus, by incorporating the energy loss into the output energy price of converter, the converter output energy price $C^{unit*}_{n,ijt}$ for per energy unit in the EH can be formulated as:

$$C^{unit*}_{n,ijt} = \frac{\sum_{f\in\Xi^F} C^{c}_{n,ft}\cdot(\mathrm{sign}(v_{n,fit}))\times\eta^{c}_{n,ij}}{\left(\sum_{j\in\Xi^J}\eta^{c}_{n,ij}\right)^2}\quad \forall i\in\Xi^I;\ \forall j\in\Xi^J;\ \forall n\in\Xi^N;\ \forall t\in\Xi^T \tag{3b}$$

Provided that each converter operates with some cost $\pi^{unit}_{n,it}$ (e.g., micro-turbine, CHP), thus the ultimate output energy price $C^{unit}_{n,ijt}$ of a converter for per energy unit becomes:

$$C^{unit}_{n,ijt} = \frac{C^{unit*}_{n,ijt}\cdot p^{unit}_{n,ijt} + \pi^{unit}_{n,it}}{p^{unit}_{n,ijt}}\quad \forall i\in\Xi^I;\ \forall j\in\Xi^J;\ \forall n\in\Xi^N;\ \forall t\in\Xi^T \tag{3c}$$

where

$$\pi^{unit}_{n,it} = \alpha_{n,i}(p^{unit}_{n,ijt})^2 + \beta_{n,i}p^{unit}_{n,ijt}\quad \forall j\in\Xi^J;\ \forall n\in\Xi^N;\ \forall t\in\Xi^T \tag{3d}$$

(2) **Collector output energy price**

The EH collector node aggregates the energy flow for a particular energy carrier, converted by converters in EH. Note that some converters only partially supply multiple energy carriers, thus the collected energy $p^{node}_{n,jt}$ for output energy carrier j at the collector node can be formulated as:

$$p^{node}_{n,jt} = \sum_{i\in\Xi^I} p^{unit}_{n,ijt}\quad \forall j\in\Xi^J;\ \forall n\in\Xi^N;\ \forall t\in\Xi^T \tag{3e}$$

Meanwhile, the output energy price of the collected energy $p^{node}_{n,j}$ at the collector node for energy carrier j can be calculated as the weighted converters output prices as:

$$C^{node}_{n,jt} = \sum_{i\in\Xi^I}\frac{C^{unit}_{n,ijt}\times p^{unit}_{n,ijt}}{p^{node}_{n,jt}}\quad \forall j\in\Xi^J;\ \forall n\in\Xi^N;\ \forall t\in\Xi^T \tag{3f}$$

(3) **ESS output energy price**

ESS, placed at the output ports of an EH, of which the charging/discharging modes can affect the output energy flow and the output energy prices of EH for different energy carriers accordingly.

(a) Assume an ESS working in the charging mode: ESS is directly supplied by the output energy of the collector node. Thus, ESS charging price $C^{ESS*}_{n,k}$ is the same as the price of the collector node.

$$C^{ESS*}_{n,kt} = \sum_{j\in\Xi^J} S_{jk}\cdot C^{node}_{n,jt}\quad \forall j\in\Xi^J;\ \forall n\in\Xi^N;\ \forall t\in\Xi^T \tag{3g}$$

However, the price of stored energy $C^{SOC}_{n,kt}$ in ESS changes with the ESS operation status, due to newly charged energy and its associated price. From this respect, $C^{SOC}_{n,kt}$ is constituted by the charged energy price (first term) and the initial cost of stored energy (second term) in the charging mode for each hour of the scheduling horizon, formulated as (3h):

$$C^{SOC}_{n,kt} = \left(\frac{P^{ch}_{n,kt}\cdot C^{ESS}_{n,kt}}{P^{ch}_{n,kt} + SOC_{n,k(t-1)}}\right) + \left(\frac{SOC_{n,k(t-1)}\cdot C^{SOC}_{n,k(t-1)}}{P^{ch}_{n,kt} + SOC_{n,k(t-1)}}\right)\quad \forall k\in\Xi^K;\ \forall n\in\Xi^N;\ \forall t\in\Xi^T \tag{3h}$$

(2) Assume an ESS working in the discharging mode: the ESS discharging price $C^{ESS*}_{n,kt}$ should be equal to the value of the price of stored energy $C^{SOC}_{n,kt}$, and $C^{SOC}_{n,kt}$ would be as the same as its original value $C^{SOC}_{n,k(t-1)}$:

$$C^{SOC}_{n,kt} = C^{SOC}_{n,k(t-1)}\quad \forall k\in\Xi^K;\ \forall n\in\Xi^N;\ \forall t\in\Xi^T \tag{3i}$$

$$C^{ESS*}_{n,kt} = C^{SOC}_{n,kt}\quad \forall k\in\Xi^K;\ \forall n\in\Xi^N;\ \forall t\in\Xi^T \tag{3j}$$

Additionally, the operation of ESS is not without cost in both charging and discharging modes [24], and the ESS operation cost ought to be transferred to its charging/discharging price. Thus, the expression of ESS charging/discharging price (in either ESS charging mode or discharging mode) can be summarized as below:

$$C^{ESS}_{n,kt} = ((P^{ch}_{n,kt} + P^{dis}_{n,kt})\cdot C^{ESS*}_{n,kt} + \pi^{ESS}_{n,kt})/(P^{ch}_{n,kt} + P^{dis}_{n,kt})\quad \forall k\in\Xi^K;\ \forall n\in\Xi^N;\ \forall t\in\Xi^T \tag{3k}$$

where

$$\pi^{ESS}_{n,kt} = \alpha_{n,k}(P^{dis}_{n,kt} - P^{ch}_{n,kt})^2 \tag{3l}$$

Note that the ESS will not simultaneously charging and discharging due to its quadratic function, of which the mathematic proof has been detailly provided in [24].

(4) **EH output energy price**

Generally, the EH operation cost, energy loss should be incorporated into the output energy price of EH output energy flow (i.e., load demand, transaction demand with other EHs and utilities). In this regard, the general formulation of the output energy price $C^{L}_{n,jt}$ of EH n for energy carrier j can be calculated as below:

$$C^{L}_{n,jt} = \left(p^{node}_{n,jt}\cdot C^{node}_{n,jt} + \sum_{k\in\Xi^K} S_{jk}\cdot(P^{dis}_{n,kt} + P^{ch}_{n,kt})\cdot C^{ESS}_{n,kt} + +\pi^{trade}_{n,jt}\right) /(P^{L}_{n,jt} + P^{ex}_{n,jt} + P^{s}_{n,jt}) \quad \forall\, j\in\Xi^J;\ \forall\, n\in\Xi^N;\ \forall\, t\in\Xi^T \tag{3m}$$

where $\pi^{trade}_{n,jt}$ denotes the operation expense that EH n exports energy to other connected EHs.

$$\pi^{trade}_{n,jt} = \alpha_{n,j} {P^{ex}_{n,jt}}^{2} \quad \forall\, j\in\Xi^J;\ \forall\, n\in\Xi^N;\ \forall\, t\in\Xi^T \tag{3n}$$

From this respect, the output energy prices $C^{L}_{n,jt}$ can be described as a function of decision vector of EH n at each time plot, i.e., $\boldsymbol{x}_{n,t}$, based on its operation and transaction strategy at time plot t, i.e.,

$$C^{L}_{n,jt} = f(\boldsymbol{x}_{n,t})\ \forall\, j\in\Xi^J;\ \forall\, n\in\Xi^N;\ \forall\, t\in\Xi^T \tag{3o}$$

Fig. 2 illustrates the general structure of inside operation scheme of a single EH and its associated output energy prices. The output energy price of each EH is developed according to the inside energy flow through the energy converters, collector nodes and ESS to meet the outside energy demands.

2.3. Individual EH operation mode

Each EH is responsible for optimizing its individual operation and transaction strategy. Based on the received information associated with inside operation cost and outside market signals (i.e., offered energy prices from the upstream energy utilities and interconnected EH systems), individual EH aims to minimize its total cost. Considering the scheduling period $t\in\Xi^T$, the objective of each hour operation scheme for EH $n\in\Xi^N$ can be formulated as follows:

$$\begin{aligned}\text{Min}\quad & \text{EH}_n(x_n)\\ = & \sum_{t\in\Xi^T}\underbrace{\left(\sum_{i\in\Xi^I}\pi^{unit}_{n,it} + \sum_{k\in\Xi^K}\pi^{ESS}_{n,kt} + \sum_{j\in\Xi^J}\pi^{trade}_{n,jt}\right)}_{\text{E1}_n}\\ & + \underbrace{\sum_{t\in\Xi^T}\sum_{f\in\Xi^F}(C^{c}_{ft}\cdot P^{c}_{ft} - C^{s}_{ft}\cdot P^{s}_{ft})}_{\text{E2}_n} +\\ & \underbrace{\sum_{t\in\Xi^T}\sum_{\forall j\in\Xi^J}\left(\sum_{m\in\Xi^{\mathcal{N}_n}} P^{im}_{nm,jt}\cdot C^{L}_{m,jt} - P^{ex}_{n,jt}\cdot C^{L}_{n,jt}\right)}_{\text{E3}_n} \quad \forall\, n\in\Xi^N\end{aligned} \tag{4}$$

where the first term E1_n covers converter, ESS and transaction operation cost; the second term E2_n represents the transaction cost with the upstream utilities; and the third term E3_n contributes to the transaction cost with other connected EH systems. Hence, the obtained total cost varies with respect to the operation and transaction strategy of the EH over the scheduling horizon. Moreover, the scheduling process of each EH is subject to the following constraints:

(1) Energy balance constraint (2)
(2) Energy dispatch and convert constraints:

$$0 \le \eta^{c}_{n,ij} \le 1 \quad \forall\, i\in\Xi^I;\ \forall\, j\in\Xi^J;\ \forall\, n\in\Xi^N \tag{5a}$$

$$0 \le v_{n,fit} \le 1 \quad \forall\, f\in\Xi^F;\ \forall\, i\in\Xi^I;\ \forall\, n\in\Xi^N \tag{5b}$$

$$\sum_{i\in\Xi^I} v_{n,fi} = 1 \quad \forall\, f\in\Xi^F;\ \forall\, n\in\Xi^N \tag{5c}$$

$$0 \le p^{unit}_{n,ijt} \le P^{unit,up}_{n,ij} \quad \forall\, j\in\Xi^J;\ \forall\, i\in\Xi^I;\ \forall\, n\in\Xi^N \tag{5d}$$

(3) ESS operation constraints:

$$SOC_{n,k} = SOC_{n,k(t-1)} + \eta^{ch}_{n,k}\cdot P^{ch}_{n,kt} - P^{dis}_{n,kt}/\eta^{dis}_{n,k} \tag{5e}$$

$$0 \le P^{ch}_{n,kt} \le P^{ch,up}_{n,k} \quad \forall\, k\in\Xi^K;\ \forall\, n\in\Xi^N \tag{5f}$$

$$0 \le P^{ch}_{n,kt} \le P^{dis,up}_{n,k} \quad \forall\, k\in\Xi^K;\ \forall\, n\in\Xi^N \tag{5g}$$

$$SOC^{\min}_{n,k} \le SOC_{n,kt} \le SOC^{up}_{n,k} \quad \forall\, k\in\Xi^K;\ \forall\, n\in\Xi^N \tag{5h}$$

(4) Transaction capacity constrains:

$$0 \le P^{c}_{n,ft} \le P^{c^{up}}_{f} \quad \forall\, f\in\Xi^F;\ \forall\, n\in\Xi^N \tag{5i}$$

$$0 \le P^{s}_{n,ft} \le P^{s^{up}}_{f} \quad \forall\, f\in\Xi^F;\ \forall\, n\in\Xi^N \tag{5j}$$

$$0 \le P^{im}_{nm,jt} \le P^{im,up}_{nm,j} \quad \forall\, j\in\Xi^J;\ \forall\, n\in\Xi^N;\ m\in\Xi^{\mathcal{N}_n} \tag{5k}$$

$$0 \le P^{ex}_{n,jt} \le P^{ex,up}_{n,j} \quad \forall\, j\in\Xi^J;\ \forall\, t\in\Xi^T \tag{5l}$$

where the constraint of (5a) represents that a non-ideal converter's efficiency is lower than 1. (5b)–(5c) guarantee the summation of the dispatch factors for the energy carrier $f\in\Xi^F$ imported from the upstream utilities is equal to one, and (5d) ensures the maximum converted energy in EH n is under the physical capacity constraints of converters. The dynamic energy balance and physic constraint for each ESS k in EH n is provided in (5e)–(5h), respectively. (5i)–(5j) guarantee the feasibility of imported/exported energy from/to upstream utilities, while (5k)–(5l) constrain the maximum transactive energy with other connected EHs. Note that if EH n and EH m is not connected by energy transmission network to transmit the energy carrier j, the value of $P^{im,up}_{nm,j}$ will be set as zero.

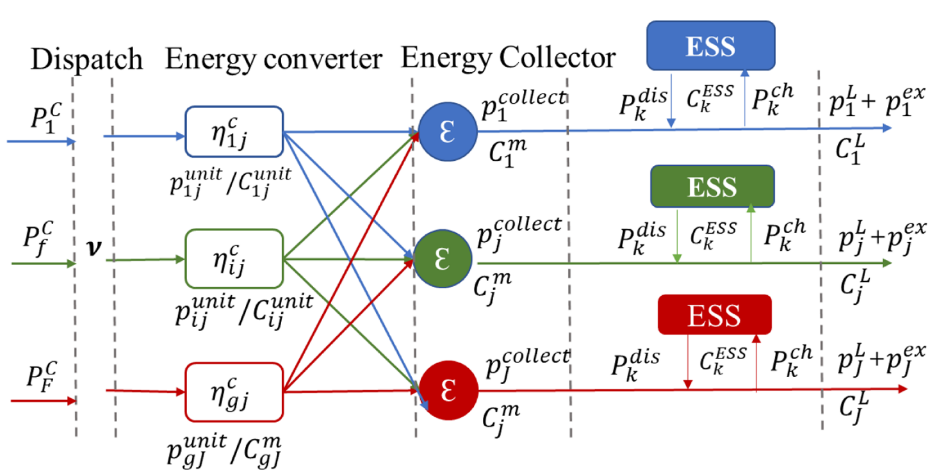

Fig. 2. The general structure of inside energy flow and output price through an EH.

2.4. Transmission network

The energy network model is composed of a group of interconnected EHs, where the transmission network connecting the EHs can be made up of electrical, thermal or hydrogen energy carriers [25]. Energy transmission loss is considered in this work, which occurs due to the energy transit process among EHs in the network for the transaction purpose. The transmission loss is approximately modeled by multiplying the transmission energy flow by a small factor l_{nm} ranging from 2% to 6%, depending on the transit distances between two interaction EH systems.

$$P_{nm,j}^{loss} = P_{nm,j}^{im} \cdot l_{nm,j} \qquad \forall j \in \Xi^J; \forall n \in \Xi^N; m \in \Xi^{\mathcal{N}_n} \tag{6}$$

Thus, although EH n intend to buy the amount of energy $P_{nm,j}^{im}$ from EH m, the actual energy received by EH n from EH m becomes:

$$P_{nm,j}^{im'} = P_{nm,j}^{im} - P_{nm,j}^{loss} \ \forall j \in \Xi^J; \forall n \in \Xi^N \tag{7}$$

Substitute (7) and into (4), the energy balance within EH n can be expressed as:

$$P_{n,jt}^{L} = \sum_{i \in \Xi^I} \left(\eta_{n,ij}^{c} \cdot \sum_{f \in \Xi^F} (\nu_{n,fit} \cdot P_{n,ft}^{c}) \right) + \sum_{k \in \Xi^K} S_{n,jk} \cdot (P_{n,kt}^{dis} - P_{n,kt}^{ch}) + P_{n,jt}^{rew} + \sum_{m \in \Xi^{\mathcal{N}_n}} (P_{nm,jt}^{im} - P_{nm,j}^{loss}) - P_{n,jt}^{ex} - P_{n,jt}^{s} \ \forall j \in \Xi^J; \forall t \in \Xi^T; \forall n \in \Xi^N \tag{8}$$

From this respect, the network energy loss between two connected EHs for the transaction is undertaken by the buyer, i.e., EH n. Moreover, the exported energy flow which is delivered from EH n ($P_{n,j}^{ex}$) will be distributed to other EHs, of which the value should equal to the summation of energy required by other EHs.

$$P_{n,j}^{ex} = \sum_{m \in \Xi^{\mathcal{N}_n}} P_{mn,j}^{im} \ \forall n \in \Xi^N \tag{9}$$

3. Problem formulation

3.1. General context

Consider EH $n \in \Xi^N$ is interconnected by other EHs by the transmission network made up of electric and thermal energy carriers. EH n can trade with adjacent EH $m \in \Xi^{\mathcal{N}_n}$ through transmission network for energy $j \in \Xi^J$ to realize its individual benefit.

The configuration of each EH system adopted in this work, constituted by three kinds of input energy carriers $f \in \Xi^F$ from the upstream network utilities (electricity upstream network P_1^C, natural gas upstream network P_2^C and heat upstream network P_3^C). The output energy carrier $j \in \Xi^J$ of each EH consist of electric carrier P_1^L and heat carrier P_2^L. Moreover, energy converters (the configuration details of electric transformer, micro-turbine, CHP and heat exchanger have been provided in Appendix A), as well as a set of electric and thermal ESSs are installed in each EH. Meanwhile a wind turbine (WT) and two solar photovoltaic (PV) system are included at EH_1, EH_2 and EH_3, respectively. A system of three interconnected EHs in Fig. 3 is to illustrate the problem formulation and general operation scenario.

In order to achieve the coordination of MEH system for global economic benefit, two categories of coordination framework in our work have been studied, i.e., the centralized framework and the decentralized framework. In the centralized mode, a system operator is responsible for the optimization of optimal energy flow amongst all EHs, while in the decentralized mode, each EH operator is in charge of its individual controllable units to participate in the local P2P market for the individual benefit.

3.2. Centralized scheduling of multi EHs system

The coordination mechanism of MEHs in centralized scheduling is provided in this section, where all the controllable energy resources in three EHs will be uniformly controlled by a centralized system operator [19] and thus the energy flow among all EHs can be determined. The centralized objective for the coordination, aiming to maximize the welfare of all EHs and minimize the transmission cost of the three interconnected EH system, can be formulated as:

$$\min \quad \sum_{t \in \Xi^T} \sum_{n \in \Xi^N} (\mathrm{E1}_n(\boldsymbol{x}_n) + \mathrm{E2}_n(\boldsymbol{x}_n)) + \sum_{n \in \Xi^N} \sum_{m \in \Xi^{\mathcal{N}_n}} \sum_{\forall j \in \Xi^J} P_{nm,jt}^{loss} \cdot C_{jt}^{c} \tag{10}$$

Subject to:

$$\mathrm{h}_j(P_n^{ex}, P_{nm}^{im}) = 0 \qquad \forall j \in \Xi^J; \forall n \in \Xi^N; m \in \Xi^{\mathcal{N}_n} \tag{11a}$$

$$\mathrm{g}_n(\boldsymbol{x}_n) = 0 \qquad \forall n \in \Xi^N \tag{11b}$$

The objective of a centralized scheme is constituted by two parts. The first part is the operation cost and transaction cost with the upstream utilities of all EHs. The second part is associated with the transmission loss, where the price for the transmission energy loss is assumed to be the same as the offered prices by the upstream utilities.

Moreover, the constraints of a centralized scheme can be divided

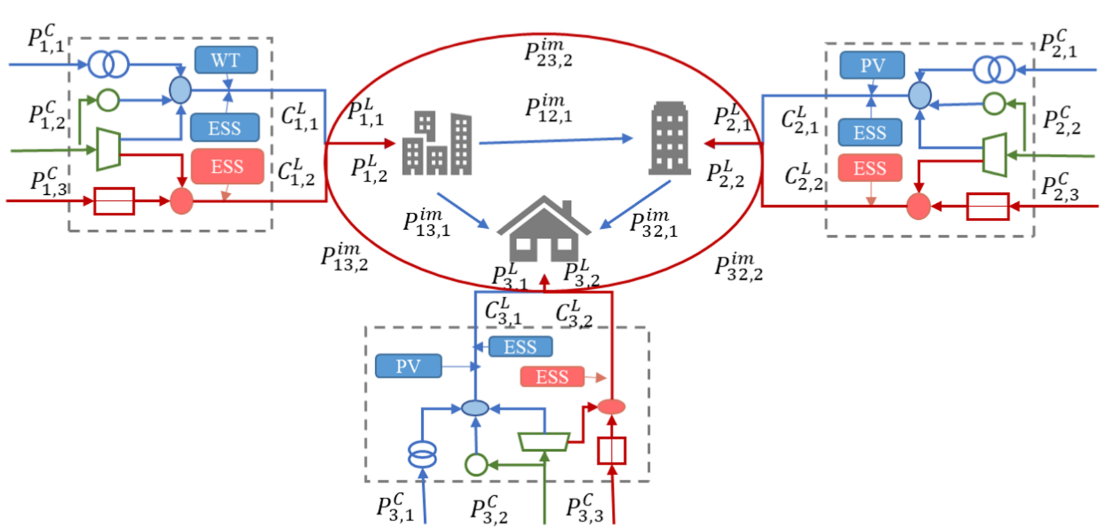

Fig. 3. Three interconnected EH system.

into two terms, i.e., the constraints of the interconnection network $h_j(\cdot)$ based on (5k), (9) for energy carrier $j \in \Xi^J$ and the constraints of individual EH n $g_n(\cdot)$, according to (5a)–(5i), (8). However, due to the nonlinear characteristics of the energy balance constraints (8) of each EH, the method in [26] is employed to linearize (8) into (A10), which will be briefly introduced in Appendix A. Thus, centralized model (10), as well as the individual EH operation model (4) can be promising solved.

3.3. Decentralized scheduling of multi EHs system

Distinct from the centralized structures, a TE based coordination framework based on P2P market platform is designed in this section for the coordination of MEHs, where two connected EHs can reach an agreement on the P2P transaction for a certain amount of energy and a price based on the local energy/information exchange. Specifically, a novel price scheme is proposed and integrated into the interaction process amongst all EHs to provide a clear market price signals, on the purpose of the realization of coordination consensus.

In this work, a modified ADMM method is utilized in the proposed TE based coordination framework, which is iteratively executed at each EH. Each iteration can be categorized into the following three stages at each time plot: (1) the EH schedule optimization stage, i.e., update $\boldsymbol{x}_n$; (2) the EH price updating stage, i.e., update C^L_n; (3) the dual variable optimization stage, i.e., update $\boldsymbol{z}_n$, where a set of auxiliary vector $\boldsymbol{z}_n = [z_{nm,j}]_{m\in\Xi^{\mathcal{N}_n}, j\in\Xi^J}$ denoting the local copy of $P^{im}_{nm,j}$ is introduced as below:

$$\begin{cases} P^{ex}_{n,j} = \sum_{m\in\Xi^{\mathcal{N}_n}} z_{mn,j} \\ P^{im}_{nm,j} = z_{nm,j} \quad ; \quad \forall j \in \Xi^J; \forall n \in \Xi^N \\ P^{im'}_{nm,j} = z_{nm,j} - P^{loss}_{nm,j} \end{cases} \tag{12a}$$

The iteration details at the τ-th iteration ($\tau \geq 1$) for time plot t can be expressed as follow:

(1) update $\boldsymbol{x}_n$

From a transaction perspective, each EH is responsible for the optimization of its individual dispatching scheme, namely the operation and transaction strategies, according to its own operation status and the limited information of other EHs. Based on received energy output prices and intended imported energy $[C^L_{m,jt}(\tau-1), P^{im}_{mn,j}(\tau-1)]_{m\in\Xi^{\mathcal{N}_n}}$ from the interconnected EH $m \in \Xi^{\mathcal{N}_n}$ at the τ-1th iteration, EH n updates its schedule by the following (12b) instead (4):

$$\begin{aligned} \boldsymbol{x}_n(\tau) &= \arg\min_{\boldsymbol{x}_n \in \mathscr{C}_n} \mathrm{M1}_n(\boldsymbol{x}_n) + \mathrm{M2}_n(\boldsymbol{x}_n) + \sum_{m\in\Xi^{\mathcal{N}_n}} (P^{im}_{nm,j} - P^{loss}_{nm,j})\cdot \\ & C^L_{m,j}(\tau-1) - P^{ex}_{n,j}\cdot C^L_{n,j}(\tau-1) + \mu \sum_{m\in\Xi^{\mathcal{N}_n}} (P^{im}_{nm,j} - z_{nm,j}(\tau-1))^2 + \mu \\ & \left(P^{ex}_{n,j} - \sum_{m\in\Xi^{\mathcal{N}_n}} z_{m,n}(\tau-1)\right)^2 \quad \forall j \in \Xi^J; \forall n \in \Xi^N \end{aligned} \tag{12b}$$

where μ is the tuning parameter, which is a positive value and can affect the convergence rate. At each iteration, the individual EH n updates (12b) by considering its constraints (A10), (5a)–(5i).

(2) update C^L_n

The output energy prices of EH n for any energy carrier $j \in \Xi^J$ are highly influenced by its EH operation and transaction strategy according to (3o). Moreover, the P2P transaction cost/benefit ought to be taken into account the output energy price generation scheme. Thus, (3o) can be modified as (12c):

$$\begin{aligned} & C^L_{n,j}(\tau) \\ & = f(\boldsymbol{x}_n(\tau)) + \frac{\sum_{m\in\Xi^{\mathcal{N}_n}} P^{im'}_{nm,j}(\tau)\cdot C^L_{m,j}(\tau-1) - P^{ex}_{n,j}(\tau)\cdot C^L_{n,j}(\tau-1)}{P^L_{n,j} + P^{ex}_{n,j}(\tau)} \quad \forall \\ & j \in \Xi^J; \forall n \in \Xi^N \end{aligned} \tag{12c}$$

(3) update $\boldsymbol{z}_n$

The $\boldsymbol{z}_n$ variable iteration process is in accordance with the market bidding mechanism. When the output energy price $C^L_{n,j}(\tau)$ of EH n exceeds the price of last iteration $C^L_{n,j}(\tau-1)$, EH n shows its tendency to export more energy, and *vice versa.* Meanwhile as the output energy price $C^L_{m,j}(\tau)$ of connected EH m exceeds the price of last iteration $C^L_{m,j}(\tau-1)$, EH n tends to decrease the imported energy from the connected EH m, and *vice versa.*

$$\begin{aligned} \boldsymbol{z}_{n,j}(\tau) = \underset{z_{nm,j}}{\mathrm{argmin}} & \mu\cdot(C^L_{m,j}(\tau) - C^L_{m,j}(\tau-1))\cdot(P^{im}_{nm,j}(\tau) - z_{nm,j}) \\ & - \mu\cdot(C^L_{n,j}(\tau) - C^L_{n,j}(\tau-1))\cdot\left(P^{ex}_{n,j}(\tau) - \sum_{m\in\Xi^{\mathcal{N}_n}} z_{mn,j}\right) \\ & + \frac{\mu}{2}(P^{im}_{nm,j}(\tau) - z_{nm,j})^2 + \frac{\mu}{2}\left(P^{ex}_{n,j}(\tau) - \sum_{m\in\Xi^{\mathcal{N}_n}} z_{mn,j}\right)^2 \\ & \forall j \in \Xi^J; \forall n \in \Xi^N \end{aligned} \tag{12d}$$

Note the updating process of EH output energy price is in parallel with the EH schedule updating process, of which the output energy price of each energy carrier $j \in \Xi^J$ is determined according to the practical operation/transaction cost and real-time imported energy prices from upstream network utilities, with clear price at each operation step of the EH. The flowchart of the TE based coordination framework for EH $n \in \Xi^N$ is shown Fig. 4.

Convergence Criterion: The convergence of the proposed decentralized model can be confirmed by each EH as the following condition is satisfied:

$$\begin{cases} |C^L_{n,j}(\tau) - C^L_{n,j}(\tau-1)| \leq \varepsilon \\ |P^{im}_{nm,j}(\tau) - P^{im}_{nm,j}(\tau-1)| \leq \varepsilon; \quad \forall j \in \Xi^J; \forall n \in \Xi^N \\ |P^{ex}_{n,j}(\tau) - P^{ex}_{n,j}(\tau-1)| \leq \varepsilon \end{cases} \tag{13}$$

where $\varepsilon > 0$ are the threshold for convergence. As each EH detects that

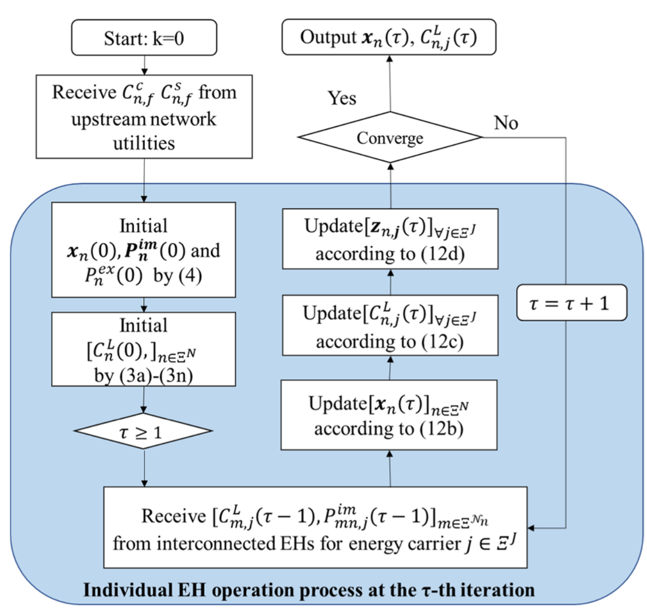

Fig. 4. The flowchart of decentralized TE-based coordination framework for EH.n

(13) for all EHs, i.e., the price and energy flow, have been satisfied, the convergence of the proposed method has been reached and the iterative process will be terminated. In other words, each EH agrees on the amount of transaction quantity and price for energy carrier $j \in \Xi^J$ with other connected EHs through iterations on the established P2P transaction platform.

4. Numerical case studies

4.1. Data setup

The proposed decentralized TE based coordination framework of MEH for the case in Fig. 3 is simulated and discussed in this section. The imported/exported energy prices from upstream utilities are illustrated in Fig. 5(a) while Fig. 5(b) and (c) present the load patterns of each EH (i.e., electric, thermal loads) and the renewable energy output, respectively. Other key setup parameters are shown in Table 1. The converters' efficiencies for transformer, micro-turbine, CHP, and heat exchanger for each EH are represented by η_{11}^c, η_{12}^c, η_{13}^c for gas to electricity and η_{23}^c for gas to heat, and η_{24}^c, respectively. The scheduling time horizon is set as one day divided into 24 one-hour time plots, i.e., T = 24, and the value of converge threshold ε , tuning parameter μ is set as 0.001 and 0.03, respectively.

4.2. Performance evaluation

In this section, the performance of the proposed decentralized TE based coordination framework for MEHs has been evaluated in terms of comprehensive perspectives, compared with other schemes presented in the literatures. Four simulation cases have been carried out, which can be defined as follows: (1) *Case A*: centralized scheme with coordination presented in Section 3.2; (2) *Case B*: decentralized scheme without coordination, in other words, individual EH optimizes its own control scheme without P2P transaction; (3) *Case C*: the proposed decentralized TE based coordination scheme through P2P transaction, i.e., the proposed method in Section 3.3; (4) *Case D*: standard ADMM decentralized scheme with coordination through P2P transaction, drawn from [20] presented in Appendix B, where a set of variables denoting transaction prices are introduced.

(1) *Economic comparison*

Table 2 reports the daily energy transactions and its associated cost obtained in these four cases. The results show that the centralized scheme in case A improve the system benefit with the lowest total fee 1835.3$, compared with other cases, i.e., 2064$ in case B, 1883.2$ in case C, and 1910.4$ in case D, respectively. However, the centralized scheme cannot avoid causing the adverse economic influence on local EH interest. For example, it increases the daily cost of EH_1 up to 808.2$ without respecting the individual EH welfare. In terms of decentralized schemes in case B, case C and case D, the decentralized scheme without P2P coordination in case B is at the highest cost. Besides, the P2P coordination scheme increases the tendency of individual EH to import more energy from grid (i.e., electricity, gas and heat energy carriers), which will be converted by EH units for transaction purpose, on condition extra benefits can be achieved. It is noticeable that the case B increases the expense of 12.5$, 124.2$, 44.1$ for EH_1, EH_2, EH_3, respectively, compared with the cost in case C, and the increase expense of 25.0$, 134.7$ for EH_1 and EH_2 compared with the cost in case D. Nearly all the EHs are individually better off when allowed to exchange energy with other EHs. However, the cost of EH_3 in case D is 850.7$, higher than its cost in case B. The main reasons can be two folds:1) the P2P transaction process is accompanied by the rising operation cost and transmission loss, which will increase the economic cost of the individual entity; 2) the decentralized scheme of a standard ADMM mode in case D requires an ultimate consensus among all entities through iterative trading interaction without considering the operation cost, which may cause benefit losses of the participants.

(2) *P2P transaction process*

Fig. 6 compares the ultimate P2P transaction prices for electricity and heat energies in the case C and case D, respectively. The energy prices obtained in these two cases show significant difference. In terms of the electricity price, the average consensus-based electricity prices of all EHs in case C (1.28$/p.u for EH1, 1.70$/p.u for EH2, 1.69$/p.u for EH3) are much lower than that in case D (1.98$/p.u for EH1, 2.03$/p.u for EH2, 2.04$/p.u for EH3) across the day. Meanwhile, the average heat prices of all EHs in case C (3.00$/p.u for EH1, 2.42$/p.u for EH2, 2.19$/p.u for EH3) are higher than that in case D (2.35$/p.u for EH1, 2.51$/p.u for EH2, 2.43$/p.u for EH3). Fig. 7 further demonstrates the P2P energy transaction quantities for electricity and heat energy in the case C and case D. In case C, the cumulative transaction electricity quantities are 79.9 p.u, 34.2 p.u, 21.7 p.u for EH_1-EH_2 transaction, EH_1-EH_3 transaction and EH_2-EH_3 transaction, respectively, while the corresponding value are 0.26.8 p.u, 1.7 p.u. and 27.13 p.u in case D. Also, the proposed TE based coordination scheme in case C can yield a bigger price gap of energy prices (i.e., electricity and heat energies) among all EHs, which further promotes individual EH to enroll in the P2P transaction scheme.

Moreover, the main reason for the price difference lies in the proposed price generation scheme in case C. The energy prices obtained by the standard ADMM in case D are highly affected by the supply-demand status in the local P2P market, where the EH price variables are updated according to the difference between the intended selling quantity of this EH and intended buying quantity of other networked EHs. However, the proposed price scheme in case C are directly derived from each EH operation and transaction decisions, denoting its real operation prices and transaction costs at each iteration. In other words, the proposed price scheme do not only adaptively change according to the P2P

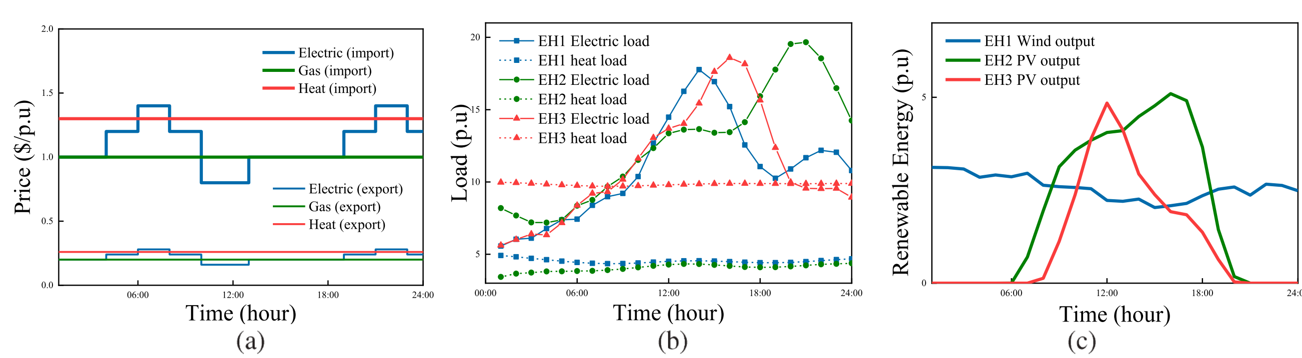

Fig. 5. the initial setting of each EH: (a) the imported/exported energy prices from upstream utility grids; (b) load patterns of each EH; (c) renewable energy output of each EH.

Table 1
Energy Hub System parameters.

Parameters		EH system: EH1	EH2	EH3
ESS $k \in \Xi^K$ of EH n	α_k	0.05	0.05	0.04
	η_k^{ch}/η_k^{dis}	0.90,0.89/0.90,0.89	0.95,0.85/0.95,0.85	0.91,0.90/0.91,0.90
	$P_k^{ch,up}/P_k^{dis,up}$	5,2/5,2	4,4/4,4	8,3/8,3
	$SOC_k^{\min}/SOC_k^{up}$	1,0.5/10,5	0.6,0.6/8,8	2,0.6/16,6
Converter $i \in \Xi^I$ of EH n	$\alpha_i\ \beta_i$	0.05/0.1	0.05/0.1	0.05/0.1
	$P_{ij}^{unit,up}$	20,15,15	20,15,15	20,15,15
	$\eta_{11}^c,\eta_{12}^c,\eta_{13}^c,\ \eta_{23}^c,\ \eta_{24}^c$	0.98,0.9,0.37,0.43,0.9	0.95, 0.9,0.4,0.4,0.95	0.99, 0.9,0.35,0.48,0.85
Transaction for energy carrier $j \in \Xi^J$ of EH n	α_j	0.05	0.05	0.05
	$P_f^{c\,up}$	20,15,15	20,15,15	20,15,15
	$P_j^{ex,up}/P_j^{\,im,up}$	8/8	8/8	8/8
Transmission loss for energy carrier$j \in \Xi^J$	$l_{12} = 4\%;\ l_{13} = 6\%;\ l_{23} = 2\%$			

market transaction status, but also reflect the instant operation cost of each EH. Table 2 also verifies the effectiveness of the proposed price scheme, where the total cost of EHs in case C is 1883.2$, lower than the cost of 1910.4$ in case D. With the respect of local interest of each EH, the better global economic performance can be achieved with the proposed TE based coordination framework in case C.

(3) *Convergence analysis*

Fig. 8 illustrates the iteration process of MEH in Case C and Case D to reach a consensus on ultimate P2P transaction energy at the time lot 18. Here, the energy deviation represents the deviation between the amount of intended exported energy of EH n and the summation of intended imported energy from EH n by the connected EH $m \in \Xi^{\mathcal{N}_n}$, i.e., $Dev_{n,j}(k) = P_{n,j}^{ex}(k) - \sum_{m\in\Xi^{\mathcal{N}_n}} P_{mn,j}^{im'}(k)$.

It is clear that the convergence is reached in both cases with good performance. The ultimate results could be obtained in 92 times of iteration to reach an equilibrium point in Case C, while it takes 76 times iteration to reach an ultimate consensus in Case D. Here the value of threshold ε for both cases is set as 0.0001. As real applications do not require such high precision, the number of iterations required can be significantly decreased.

(4) *Energy price analysis*

According to the above results pertaining to the value of energy carriers and the associated upstream prices, ESS operation, renewable energy output and transaction strategies, the output energy prices of EH at each operation step are presented by Fig. 9 for both the electricity and heat output energy carriers on the basis of our proposed EH output price generation scheme. The inner operation price (collector node C^{node}, ESS C^{ESS}) and output energy price (C^L) of each EH are demonstrated accordingly.

In general, the collector output energy prices for both electricity and heat energy carriers are higher than the ultimate EH output energy prices for all EHs across the day. Particularly, the difference of average EH output prices and collector output prices for electricity can reach to 0.60 $/p.u, 0.51$/p.u, and 0.26$/p.u for EH1, EH2 and EH3, respectively. The primary reason is that the equipped renewable energy generators (i.e., PV and WT) in each EH produce electricity without additional operation fee, which affects EH prices in two ways. On the one hand, it significantly decreases the EH output electricity price according to the specific supply-demand status of each EH. That further stimulates other networked EHs to import energy from the EHs offering the relatively low energy prices. For example, the obtained EH1 output electricity price from 0:00am to 10:00am is even lower than the offered price of the upstream electric utility, presented in Fig. 5. Therefore, EH2 and EH3 undoubtedly prefer to import electricity from EH1 during this period, as shown in Fig. 7. On the other hand, the flexible conversion process of the EH intensifies the coupling energy-price relationship of different energy carriers. Thus, the decreasing EH output electricity price further helps to reduce the output heat price of this EH to a certain

Table 2
Performance comparison among four cases.

Case		Energy imported (p.u)					Energy exported (p.u)				Trading Fee ($)	Operation Fee ($)	Total Fee ($)
		From Grid			From other EHs		To Grid		To Other EHs				
		Electric	Gas	Heat	Electric	Heat	Electric	Heat	Electric	Heat			
Case A	EH_1	222.8	184.7	142.7	1.6	0.8	0	8.5	91.2	93.4	512.5	295.6	808.2
	EH_2	184.7	127.1	86.8	35.8	0.0	0	0	8.0	38.8	447.6	124.1	571.7
	EH_3	142.7	86.8	76.4	65.6	131.4	0	0	2.1	1.2	343.7	111.7	455.4
Case B	EH_1	161.0	102.1	69.9	~		0	0	~		366.6	166.9	533.5
	EH_2	212.9	127.8	47.9			0	2.1			431.5	254.4	685.9
	EH_3	169.5	185.7	170.3			0	0			593.9	250.5	844.6
Case C	**EH_1**	**239.5**	**122.2**	**48.2**	**29.1**	**12.9**	**0**	**0**	**105.0**	**0.1**	**373.7**	**147.3**	**521.0**
	EH_2	**187.7**	**131.1**	**117.6**	**81.1**	**0.0**	**0**	**0**	**50.6**	**65.7**	**430.6**	**131.1**	**561.7**
	EH_3	**144.9**	**153.9**	**129.5**	**57.5**	**52.8**	**0**	**0**	**12.5**	**0.1**	**612.2**	**188.3**	**800.5**
Case D	EH_1	185.6	96.7	101.8	5.2	0.0	0	0	23.3	26.6	329.5	179.0	508.5
	EH_2	198.0	95.0	112.8	45.4	0.5	0	0	14.3	50.2	406.2	145.1	551.2
	EH_3	207.5	122.0	118.3	10.7	76.3	0	0	24.0	2.4	661.1	189.6	850.7

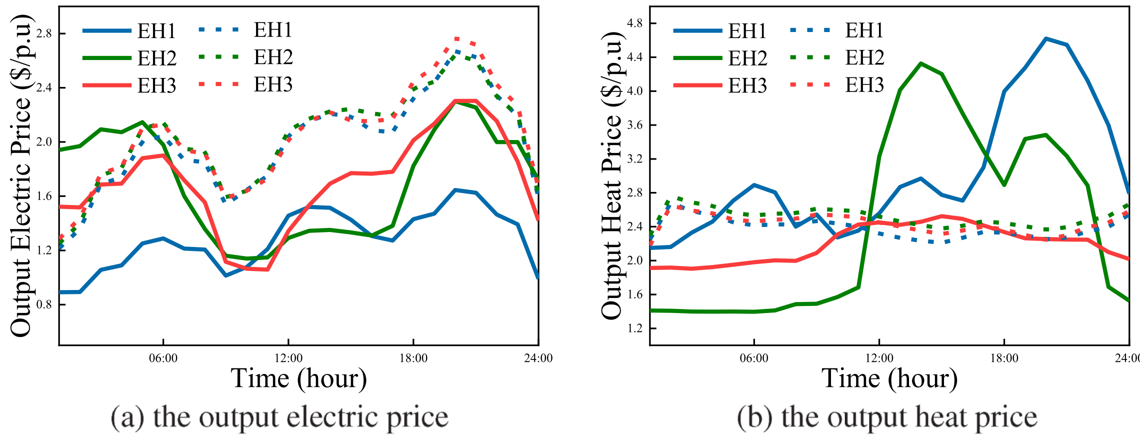

Fig. 6. The ultimate energy transaction prices of each EH in case C and case D across the day. (solid lines represent the simulation results in Case C and short dash lines represent the simulation results in Case D).

degree.

Additionally, it is noticeable that the value of ESS charging/discharging prices are generally the same as the collector node for the most hours in a day. That is because there are no changing/discharging actions of ESS during these hours. However, as ESS charge energy from the collector node, its price slightly increases due to the additional operation cost, compared with the collector price (for example, the price of EH1 during the 0:00 am and 4:00 am). But, as ESS operates in a discharge mode, a sudden price drop will appear. The reason is that the ESS charging/discharging price equals to the price of the stored energy in the ESS, rather than the collector node. In general, the ESS intends to charge during the hours with relatively low EH output energy price to supplement its stored energy and discharge as the EH output energy price increases for the maximization of EH benefit.

Apart from renewable energy generation, EH output energy prices can also be affected by two other factors, i.e., the prices from upstream utilities (especially for electricity) and its inner energy demands. Fig. 9 reveals that the EH output electricity prices show the similar variation tendency as the electric load pattern during the consumption peak hours (in the afternoon and at night). That is the highest EH output electricity prices appear at the time with peak electric consumption. Specifically, although the heat loads of all EH are generally flat, as indicated in Fig. 5(b), the EH output heat prices show a great increase during the electricity peak hours. It is because more heat energy imported from the upstream utilities is converted to the electricity so as to satisfy the electric load and transaction demand, which results in the higher operation cost and EH output heat prices. Moreover, during non-peak hours (in the morning), the EH output energy prices generally follow the variation tendency of the energy prices from upstream utilities.

In this regard, the proposed EH price scheme tightly couple various energy carriers and upstream utilities, providing transparent price signals in the local P2P market. The provided consensus-based transaction price do not only encloses the information of supply-demand status in the local P2P market (for example, the high energy price during peak hours and relatively low energy price during non-peak hours), but also actively stimulates each entity to autonomously interact with networked EHs on the basis of individual benefits.

5. Conclusion

The paper proposes a decentralized transaction-based energy management for the coordination of connected multiple energy hubs integrated with multiple energy carriers. A generic framework based on peer to peer energy transaction is developed to depict the conversion, storage, transaction process of MEH system with specific energy prices at each operation step, which can comprehensively reflect the correlation of EH operation and transaction strategy with EH output energy prices. Specifically, the output energy prices change in line with each EH operation strategy, which is integrated into a modified ADMM method to facilitate the coordination and consensus-reaching process amongst EHs on the peer to peer transaction platform. Numerical case

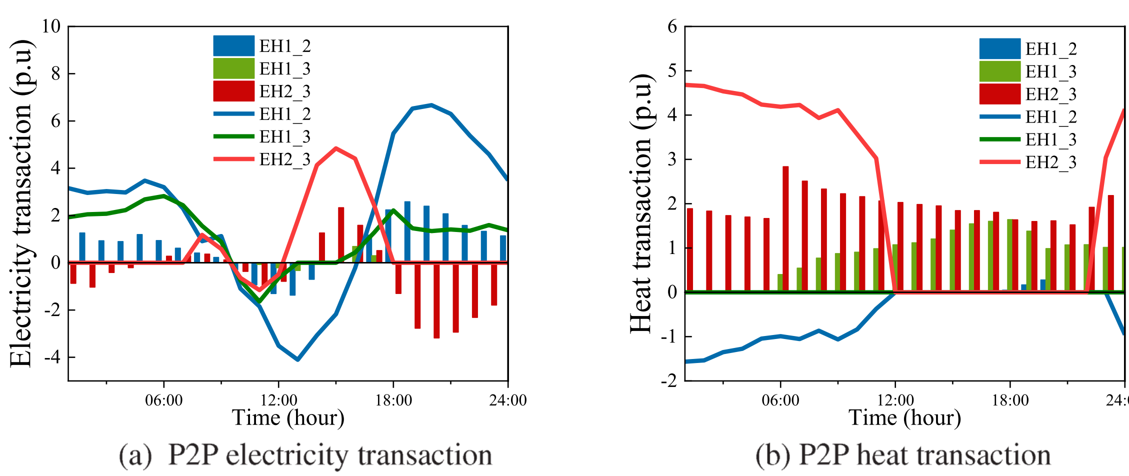

Fig. 7. The ultimate energy transaction amount among EHs in case C and case D across the day, where solid lines represent the simulation results in case C and bar graph represent the simulation results in case D. Note that EH1-2 represents the energy flow between EH_1 and EH_2. A positive value represents EH1 export energy to EH2, and the negative value *vice versa*.

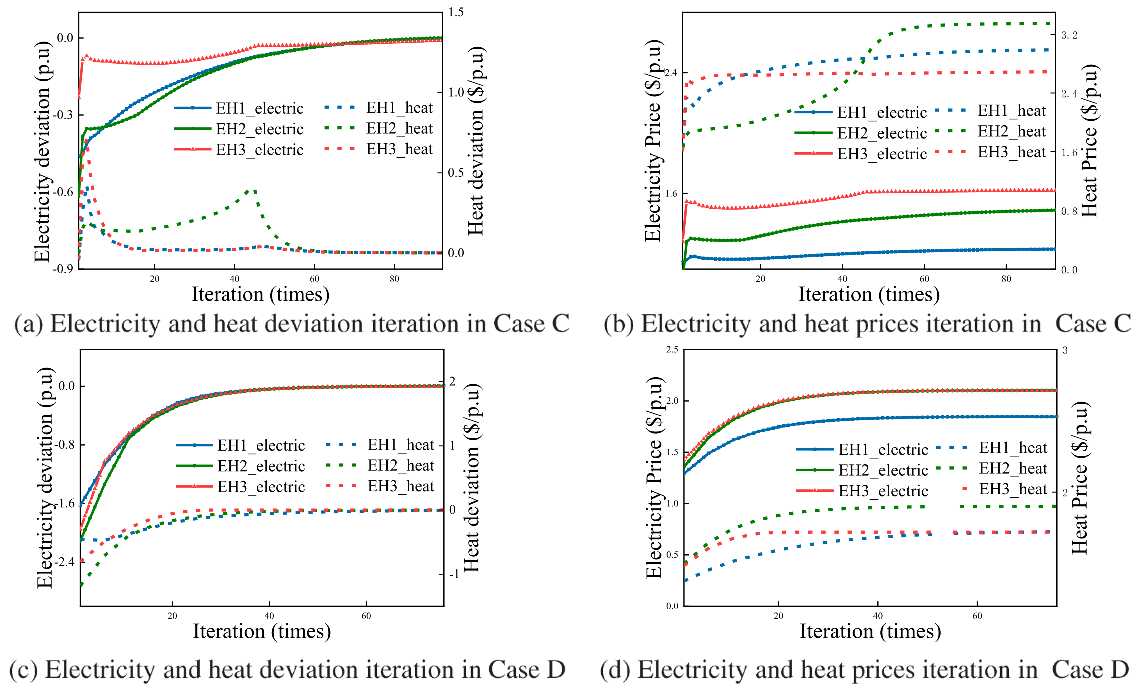

(a) Electricity and heat deviation iteration in Case C (b) Electricity and heat prices iteration in Case C

(c) Electricity and heat deviation iteration in Case D (d) Electricity and heat prices iteration in Case D

Fig. 8. Iteration process of energy deviation and prices in Case C and Case D.

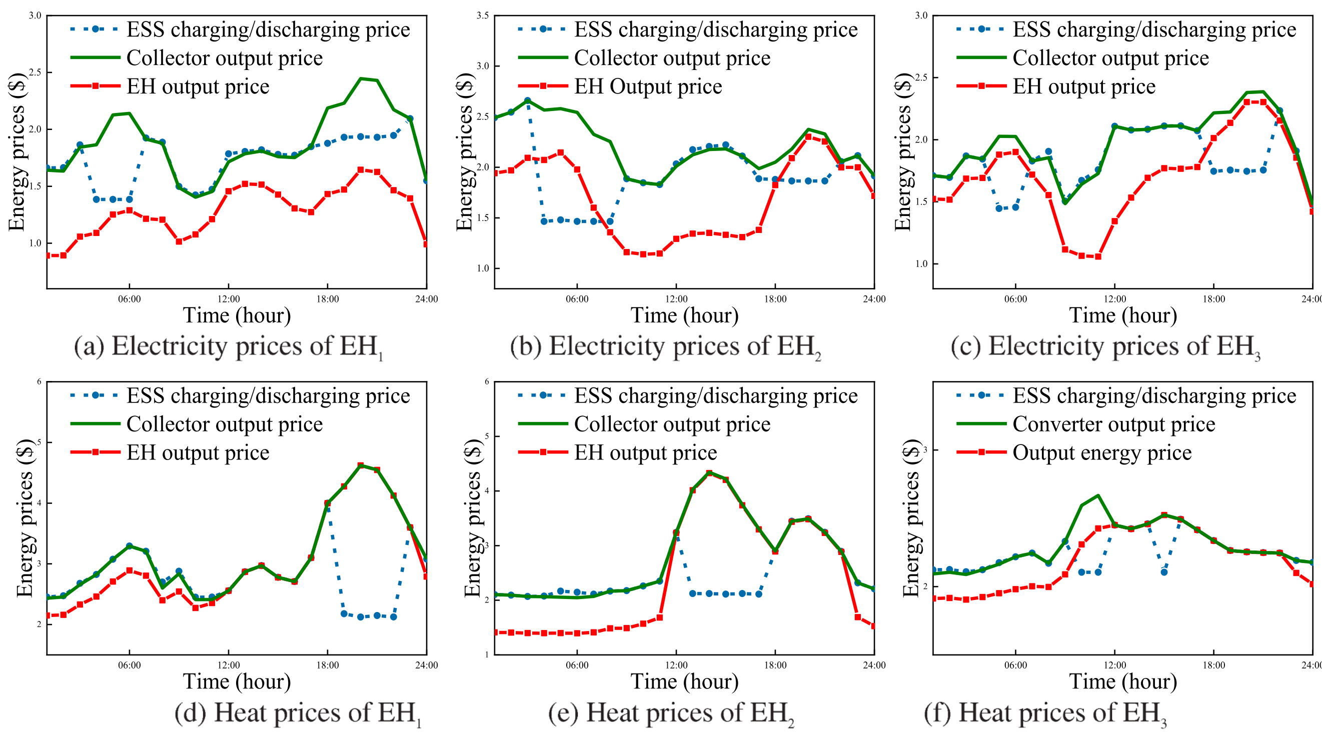

(a) Electricity prices of EH_1 (b) Electricity prices of EH_2 (c) Electricity prices of EH_3

(d) Heat prices of EH_1 (e) Heat prices of EH_2 (f) Heat prices of EH_3

Fig. 9. Energy prices of each EH across the day.

studies have been carried out and the simulation results show that the proposed model can achieve optimal economic benefits from both local and global perspectives, compared with alternative schemes. Future work focuses on incorporating other optimization schemes, e.g., demand response, into multiple EHs optimization process.

CRediT authorship contribution statement

Xiaodi Wang: Formal analysis, Writing - original draft. **Youbo Liu:** Validation, Writing - review & editing. **Chang Liu:** Validation, Writing - review & editing. **Junyong Liu:** Supervision, Funding acquisition.

Declaration of Competing Interest

The authors declare that they have no known competing financial interests or personal relationships that could have appeared to influence the work reported in this paper.

Acknowledgements

This research was supported by National Key R&D Program of China (Grant No. 2017YFE0112600).

Appendix A

The inner configuration of each EH descripted in Section 3.1 can be formulated as:

$$\boldsymbol{P_n^C} = \begin{bmatrix} P_{n,1}^C \\ P_{n,2}^C \\ P_{n,F}^C \end{bmatrix} \quad \boldsymbol{\nu_n} = \begin{bmatrix} 1 & 0 & 0 \\ 0 & \nu_{n,22} & 0 \\ 0 & \nu_{n,23} & 0 \\ 0 & 0 & 1 \end{bmatrix} \quad \boldsymbol{P_n^L} = \begin{bmatrix} P_{n,1}^L \\ P_{n,2}^L \end{bmatrix} \quad \boldsymbol{\eta_n} = \begin{bmatrix} \eta_{n,11}^c & \eta_{n,12}^c & \eta_{n,13}^c & 0 \\ 0 & 0 & \eta_{n,23}^c & \eta_{n,24}^c \end{bmatrix} \tag{A1}$$

The feasible space of individual EH is defined by (5a)–(5o) which can be expressed as the linear functions of decision variables $\boldsymbol{x}_n = [[P_f^c]_{f\in\Xi^F}, [\nu_{fit}]_{f\in\Xi^F, i\in\Xi^I}, [P_{n,k}^{ch}, P_{n,k}^{dis}]_{k\in\Xi^K}, [P_{n,j}^{ex}, P_{n,j}^{s}]_{j\in\Xi^J}, [P_{nm,j}^{im}]_{j\in\Xi^J, m\in\Xi^{\mathcal{N}n}}]$, except the power balance equations in (8). More specifically, without considering ESS and interconnected transaction, the energy balance is

$$\begin{bmatrix} P_{n,1}^L \\ P_{n,2}^L \end{bmatrix} = \begin{bmatrix} \eta_{n,11}^c & \eta_{n,12}^c & \eta_{n,13}^c & 0 \\ 0 & 0 & \eta_{n,23}^c & \eta_{n,24}^c \end{bmatrix} \times \begin{bmatrix} 1 & 0 & 0 \\ 0 & \nu_{n,22} & 0 \\ 0 & \nu_{n,23} & 0 \\ 0 & 0 & 1 \end{bmatrix} \times \begin{bmatrix} P_{n,1}^C \\ P_{n,2}^C \\ P_{n,3}^C \end{bmatrix} \tag{A2}$$

And we have

$$P_{n,1}^L = \eta_{n,11}^c P_{n,1}^C + \nu_{n,22}\eta_{n,12}^c P_{n,2}^C + \nu_{n,23}\eta_{n,13}^c P_{n,2}^C \tag{A3}$$

$$P_{n,2}^L = \nu_{n,23}\eta_{n,23}^c P_{n,2}^C + \eta_{n,24}^c P_{n,3}^C \tag{A4}$$

Subject to

$$\nu_{n,22} + \nu_{n,23} = 1 \tag{A5}$$

Eqs. (A2) − (A5) are nonlinear functions of decision variables $\nu_{n,22} + \nu_{n,23}$, submitting $\nu_{n,23} = 1 - \nu_{n,22}$ into **(A3) and (A4)**, we obtain

$$P_{n,1}^L = \eta_{n,11}^c P_{n,1}^C + \nu_{n,22}\eta_{n,12}^c P_{n,2}^C + (1-\nu_{n,22})\eta_{n,13}^c P_{n,2}^C \tag{A6}$$

$$P_{n,2}^L = (1-\nu_{n,22})\eta_{n,23}^c P_{n,2}^C + \eta_{n,24}^c P_{n,3}^C \tag{A7}$$

From (A7) we have

$$\nu_{n,22} = \frac{1}{\eta_{n,23}^c P_{n,2}^C}(\eta_{n,23}^c P_{n,2}^C + \eta_{n,24}^c P_{n,3}^C - P_{n,2}^L) \tag{A8}$$

Integrate (A8) into (A6), we get

$$P_{n,1}^L = \eta_{n,11}^c P_{n,1}^C + \eta_{n,13}^c P_{n,2}^C + \frac{\eta_{n,13}^c - \eta_{n,12}^c}{\eta_{n,23}^c}(P_{n,2}^L - \eta_{n,23}^c P_{n,2}^C - \eta_{n,24}^c P_{n,3}^C) \tag{A9}$$

Equation (A9) become a linear function of decision variables $[P_f^c]_{f\in\Xi^F}$. Moreover, the ESS and transaction operation scheme of an EH are a strictly convex models, of which the constraints are linear as integrated into the constraint (A9). Thus, the nonlinear energy balance constraint (8) can be rewritten as the linear equality constraint form (A10).

$$P_{n,1}^L = \eta_{n,11}^c P_{n,1}^C + \eta_{n,13}^c P_{n,2}^C + \frac{\eta_{n,13}^c - \eta_{n,12}^c}{\eta_{n,23}^c}(P_{n,2}^L - \eta_{n,23}^c P_{n,2}^C - \eta_{n,24}^c P_{n,3}^C) + P_{n,1}^{dis} - P_{n,1}^{ch} + P_{n,1}^{rew} + \sum_{m\in\Xi^{\mathcal{N}n}}(P_{nm,1}^{im} - P_{nm,1}^{loss}) - P_{n,1}^{ex} \tag{A10}$$

Appendix B

The optimization problem of (4) is

$$\text{Min} \quad \text{EH}_n(\boldsymbol{x}_n) \tag{B1}$$

Introduction a set of vectors $\boldsymbol{z_n} = [z_{nm,j}]_{m\in\Xi^{\mathcal{N}n}, j\in\Xi^J}$ representing the local copy of $P_{nm,j}^{im}$ as (12a) and $\boldsymbol{\lambda}_n = [\lambda_{nm,j}]_{n\in\Xi^N, m\in\Xi^{\mathcal{N}n}, j\in\Xi^J}$ a set of auxiliary vector denoting the transaction prices as the Lagrangian multiplier vector.

Thus, the augmented Lagrange function of (B1) can be defined as

$$\mathscr{L}_{n,j}(\boldsymbol{x}, \boldsymbol{\lambda}, \boldsymbol{z}) = \sum_{n\in\Xi^N}\left[\text{EH}_n(\boldsymbol{x}_n) + \sum_{j\in\Xi^J}\sum_{m\in\Xi^{\mathcal{N}n}}\lambda_{mn,j}(P_{nm,j}^{im} - z_{nm,j}) - \lambda_{nn,j}\left(P_{n,j}^{ex} - \sum_{m\in\Xi^{\mathcal{N}n}} z_{mn,j}\right) + \frac{\mu}{2}\sum_{m\in\Xi^{\mathcal{N}n}}(P_{nm,j}^{im} - z_{nm,j})^2 + \frac{\mu}{2}\left(P_{n,j}^{ex} - \sum_{m\in\Xi^{\mathcal{N}n}} z_{mn,j}\right)^2\right] \quad \forall j\in\Xi^J; \forall n\in\Xi^N \tag{B2}$$

The standard ADMM update $\boldsymbol{x}$, $\boldsymbol{z}$, $\boldsymbol{\lambda}$ as

(1) update $\boldsymbol{x}$

$$\boldsymbol{x}_n(k) = \arg\min_{\boldsymbol{x}_n \in \mathscr{C}_{\boldsymbol{n}}} \mathrm{EH}_n(\boldsymbol{x}_n) + \sum_{j\in\Xi^J}\sum_{m\in\Xi^{\mathscr{N}_n}} \lambda_{mn,j}(k-1)P^{im}_{nm,j} - \lambda_{nn,j}P^{ex}_{n,j} + \frac{\mu}{2}\sum_{m\in\Xi^{\mathscr{N}_n}}(P^{im}_{nm,j} - z_{nm,j}(k-1))^2 + \frac{\mu}{2}\left(P^{ex}_{n,j} - \sum_{m\in\Xi^{\mathscr{N}_n}} z_{mn,j}(k-1)\right)^2 \quad \forall j\in\Xi^J;\ \forall n\in\Xi^N \tag{B3}$$

(2) update $\boldsymbol{z}$

$$\boldsymbol{z_n}(k) = \operatorname*{argmin}_{z_{nm,j}} \boldsymbol{\lambda}_{nn,j}(k-1)z_{nm,j} - \boldsymbol{\lambda}_{nm,j}(k-1)z_{mn,j} + \frac{\mu}{2}(P^{im}_{mn,j}(k) - z_{mn,j})^2 + \frac{\mu}{2}\left(P^{ex}_{n,j}(k) - \sum_{m\in\Xi^{\mathscr{N}_n}} z_{mn,j}\right)^2 \quad \forall j\in\Xi^J;\ \forall n\in\Xi^N \tag{B4}$$

(3) update $\boldsymbol{\lambda}$

$$\boldsymbol{\lambda}_{nn,j}(k) = \boldsymbol{\lambda}_{nn,j}(k-1) - \mu\left(P^{ex}_{n,j}(k) - \sum_{m\in\Xi^{\mathscr{N}_n}} z_{mn,j}\right); \quad \forall j\in\Xi^J;\ \forall n\in\Xi^N \tag{B5}$$

$$\boldsymbol{\lambda}_{mn,j}(k) = \boldsymbol{\lambda}_{mn,j}(k-1) + \mu(P^{im}_{nm,j}(k) - z_{nm,j}) \quad \forall j\in\Xi^J;\ m\in\Xi^{\mathscr{N}_n};\ \forall n\in\Xi^N \tag{B6}$$

Thus, it is straightforward to show that the analytical solution of (B4) satisfies

$$P^{im}_{mn,j}(k) - z_{mn,j}(k) + P^{ex}_{n,j}(k) - \sum_{m\in\Xi^{\mathscr{N}_n}} z_{mn,j}(k) = \frac{1}{\mu}[\lambda_{nn,j}(k-1) - \lambda_{nm,j}(k-1)] \tag{B7}$$

Leading to

$$\lambda_{nn,j}(k-1) = \lambda_{nm,j}(k-1) \tag{B7}$$

Since the scheduling problem (B1) is convex, the ADMM algorithm is guaranteed to converge to the optimal solution of (B1).

References

[1] Zhang X, Shahidehpour M, Alabdulwahab A, Abusorrah A. Optimal expansion planning of energy hub with multiple energy infrastructures. IEEE Trans Smart Grid 2015;6(5):2302–11.
[2] Ma L, Liu N, Zhang J, Wang L. Real-time rolling horizon energy management for the energy-hub-coordinated prosumer community from a cooperative perspective. IEEE Trans Power Syst 2019;34(2):1227–42.
[3] Majidi M, Nojavan S, Zare K. A cost-emission framework for hub energy system under demand response program. Energy 2017;134:157–66.
[4] Derafshi Beigvand S, Abdi H, La Scala M. A general model for energy hub economic dispatch. Appl Energy 2017;190:1090–111.
[5] Dolatabadi A, Mohammadi-Ivatloo B. Stochastic risk-constrained scheduling of smart energy hub in the presence of wind power and demand response. Appl Therm Eng 2017;123:40–9.
[6] Holjevac N, Capuder T, Zhang N, Kuzle I, Kang C. Corrective receding horizon scheduling of flexible distributed multi-energy microgrids. Appl Energy 2017;207:176–94.
[7] Najafi A, Falaghi H, Contreras J, Ramezani M. 'A stochastic bilevel model for the energy hub manager problem'. IEEE Trans Smart Grid 2017;8(5):2394–404.
[8] Essayeh Chaimaa, El Fenni Mohammed Raiss, Dahmouni Hamza. Optimizationofenergyexchangein microgridnetworks:acoalitionformation approach. Prot Control Mod Power Syst 2020;1:1–20.
[9] Wang X, et al. Thermally controllable demand response with multiple load aggregators. Electr Power Syst Res 2020;179:106102.
[10] Huang Zhao, Fang Baling, Deng Jin. Multi-objective optimization strategy for distribution network considering V2Genabledelectric vehicles in building integrated energy system. Prot Control Mod Power Syst 2020;1:48–55.
[11] Liu Y, Zuo K, Liu X, Liu J, Kennedy JM. Dynamic pricing for decentralized energy trading in micro-grids. Appl Energy 2018;228:689–99.
[12] Hug G, Kar S, Wu C. Consensus + Innovations approach for distributed multi-agent coordination in a microgrid. IEEE Trans Smart Grid 2015;6(4):1893–903.
[13] Liu N, Yu X, Wang C, Li C, Ma L, Lei J. Energy-sharing model with price-based demand response for microgrids of peer-to-peer prosumers. IEEE Trans Power Syst 2017;32(5):3569–83.
[14] Kang J, Yu R, Huang X, Maharjan S, Zhang Y, Hossain E. Enabling localized peer-to-peer electricity trading among plug-in hybrid electric vehicles using consortium blockchains. IEEE Trans Ind Inform Dec. 2017;13(6):3154–64.
[15] Majumder BP, Faqiry MN, Das S, Pahwa A. An efficient iterative double auction for energy trading in microgrids. In: Proc. IEEE Symp. Comput. Intell. Appl. Smart Grid, Orlando, FL, USA, 2014, p. 1–7.
[16] Wang Z, Chen B, Wang J, Begovic MM, Chen C. Coordinated Energy Management of Networked Microgrids in Distribution Systems. IEEE Trans Smart Grid 2015;6(1):45–53.
[17] Liu Y, et al. Dynamic pricing for decentralized energy trading in micro-grids. Appl Energy 2018;228:689–99.
[18] Fan S, Li Z, Wang J, Piao L, Ai Q. Cooperative Economic Scheduling for Multiple Energy Hubs: A Bargaining Game Theoretic Perspective. IEEE Access 2018;6:27777–89.
[19] Liu W, Zhan J, Chung CY. A novel transactive energy control mechanism for collaborative networked microgrids. IEEE Trans Power Syst 2019;34(3):2048–60.
[20] Liu Y, et al. Distributed robust energy management of a multi microgrid system in the real-time energy market. IEEE Trans Sustain Energy 2019;10(1):396–406.
[21] Liu Y, Gooi HB, Li Y, Xin H, Ye J. A Secure Distributed Transactive Energy Management Scheme for Multiple Interconnected Microgrids Considering Misbehaviors. IEEE Trans Smart Grid 2019;10(6):5975–86.
[22] Aghamohamadi Mehrdad, Samadi Mahdi, Rahmati Iman. Energy generation cost in multi-energy systems; an application to a non-merchant energy hub in supplying price responsive loads. Energy 2018;161:878–91.
[23] Davatgaran Vahid, Saniei Mohsen, Mortazavi Seyed Saeidollah. Smart distribution system management considering electrical and thermal demand response of energy hubs. Energy 2019;169:38–49.
[24] Wu D, Yang T, Stoorvogel AA, Stoustrup J. Distributed Optimal Coordination for Distributed Energy Resources in Power Systems. IEEE Trans Automation Science and Engineering 2017;14(2):414–24.
[25] Huo D, Gu C, Ma K, Wei W, Xiang Y, Le Blond S. Chance-Constrained Optimization for Multienergy Hub Systems in a Smart City. IEEE Trans Industrial Electronics 2019;66(2):1402–12.
[26] Bahrami S, Toulabi M, Ranjbar S, Moeini-Aghtaie M, Ranjbar AM. A Decentralized Energy Management Framework for Energy Hubs in Dynamic Pricing Markets. IEEE Trans Smart Grid 2018;9(6):6780–92.